LAMINAR TRANSPORT PHENOMENA IN CONSTRICTED PARALLEL DUCTS

Sahas Bunditkul and Wen-Jei Yang
Department of Mechanical Engineering
The University of Michigan, Ann Arbor, Michigan 48109

(Communicated by J.P. Hartnett and W.J. Minkowycz)

ABSTRACT
       A finite-difference numerical method is developed to solve heat and
       momentum transfer problems in viscous, incompressible, laminar flow
       through parallel ducts with abrupt contraction and enlargement. Con-
       sideration is given to two limiting thermal conditions: constant wall
       temperature and constant wall heat flux. Theoretical results are ob-
       tained for the loss coefficients due to abrupt contraction and ex-
       pansion, heat transfer performance and combined hydrodynamic and ther-
       mal entrance length. The effects of the flow-area variation, thermal
       boundary conditions, and Reynolds and Prandtl number on the contrac-
       tion and expansion coefficients, entrance length, and local and average
       Nusselt number are determined. The present numerical scheme is cap-
       able of producing results for the complex channel flows up to the
       transition Reynolds number. It is disclosed that the flow constric-
       tions cause a substantial enhancement in heat transfer.

Introduction

   The problems of momentum and heat transfer in laminar flows through long

passages including the entrance region have been thoroughly treated and their

theoretical and empirical results are well documented, for example reference 1.

However, owing to mathematical complexity, only limited effort has been de-

voted to hydrodynamic behavior [2-9] and none to thermal characteristics in

internal flows with abrupt enlargements and contractions. The knowledge is

nevertheless of great importance to the design of piping systems, heat exchange

devices and artificial cardiovascular systems.

Kays [2] has obtained semi-empirical results on the expansion and con-
traction coefficients, K_e and K_c respectively, for flows through tubes and
ducts with abrupt constrictions. These loss coefficients whose magnitude is
a measure of pressure drop Δp^* due to abrupt expansion or contraction can be
determined from the Darcy equation

$$\Delta p^* = K\rho (V^*)^2 / (2g_c) \tag{1}$$

Here, ρ denotes the fluid density, V^*, the bulk velocity inside the flow pas-
sage, and g_c, the conversion factor. His results are applicable to only the
flow passage of large length-to-hydraulic diameter ratio L^*/D_h^*, since the study
was performed on a fully-developed flow in either the laminar or turbulent
range. This is evidenced by a single curve in the $K-\sigma$ plot for the laminar
range having the Reynolds number Re less than 2000. σ represents the ratio of
free-flow area to frontal area. Benedict et al [3] have extended the study
on the loss coefficients to compressible and constant-density fluids including
applications to typical globe valves and associated piping systems [4]. Num-
erical studies have been performed on viscous, incompressible flow through an
orifice in a circular tube using the methods of finite differences [5] and
finite elements [6]. The Poiseuille velocity profile has been imposed both at
the entrance and exit of the tube. Flow profiles have been obtained for the
Reynolds numbers up to 500. The separation vortex is seen at downstream of a
constricted step. Flows of a viscous incompressible fluid through axisymmetric
circular ducts of variable axial geometry have been conducted for applications
to cardiovascular flow systems including arterial stenoses [7,8] and the aortic
valve [9]. It is disclosed in reference 9 by a finite-difference numerical
method that a vorticity is formed and grows in a spherical cavity during the
accelerating-flow phase.

While the flow profiles and pressure losses in constricted flow passages
have been fairly well studied no effort has ever been directed toward heat
transfer problems in such a flow system.

In the present paper, a finite-difference numerical method is employed
to study heat and momentum transfer in laminar flows through constricted par-
allel ducts. Results are compared with those for a parallel duct.

Analysis

Consider a viscous, incompressible flow through a parallel channel of

width a^* with a rectangular constriction of width b^* and length L^* situated at a distance L_1^* from the channel entrance, as shown in Fig. 1. The channel ends at a distance L_2^* downstream of the step. The flow is laminar and fully developed as it enters the channel, while only the walls of the constriction are heated. The constriction is of sufficient length so that there is an essentially fully developed velocity profile at the exit. The flow is then disrupted again at the abrupt enlargement. The case of short channels will be treated in a separate paper.

The vorticity, continuity, momentum and energy equations in dimensionless form read

$$u \frac{\partial \omega}{\partial x} + v \frac{\partial \omega}{\partial y} = C \frac{\partial^2 \omega}{\partial x^2} + \frac{\partial^2 \omega}{\partial y^2} \tag{2}$$

$$\frac{\partial u}{\partial x} + \frac{\partial v}{\partial y} = 0 \tag{3}$$

$$u \frac{\partial u}{\partial x} + v \frac{\partial u}{\partial y} = -C \frac{\partial P}{\partial x} + C \frac{\partial^2 u}{\partial x^2} + \frac{\partial^2 u}{\partial y^2} \tag{4-a}$$

$$u \frac{\partial v}{\partial x} + v \frac{\partial v}{\partial y} = - \frac{\partial P}{\partial y} + C \frac{\partial^2 v}{\partial x^2} + \frac{\partial^2 v}{\partial y^2} \tag{4-b}$$

$$u \frac{\partial T}{\partial x} + v \frac{\partial T}{\partial y} = \frac{1}{Pr} (C \frac{\partial^2 T}{\partial x^2} + \frac{\partial^2 T}{\partial y^2}) \tag{5}$$

respectively. Here, the origin of the Cartesian coordinates (x,y) is fixed at the channel entrance with x measuring the distance in the flow direction, as shown in Fig. 1. u, v, ω, P and T denote the x- and y- direction velocity components, vorticity, pressure and temperature, respectively. C is defined as $(b^*/L^*)^2$. The continuity equation (3) can be satisfied by the use of the stream function ψ defined as

$$u = \partial \psi / \partial y, \qquad v = -\partial \psi / \partial x \tag{6}$$

Then the vorticity reads

$$\omega = C \frac{\partial^2 \psi}{\partial x^2} + \frac{\partial^2 \psi}{\partial y^2} \tag{7}$$

The appropriate boundary conditions are specified as follows: the flow at the inlet x = 0 is fully developed, that is, $u = \frac{3}{2} \bar{u}[1-(\frac{2y}{a})^2]$, v = 0, $\psi = \frac{3}{2} \bar{u}[1- \frac{1}{3}(\frac{2y}{a})^2]y$ and $\omega = -12\bar{u} y/a^2$, where $\bar{u}$ is the mean velocity over the channel cross section. Along the walls including the corners, one has zero velocity components, constant stream function and $C \frac{\partial^2 \omega}{\partial x^2} + \frac{\partial^2 \omega}{\partial y^2} = 0$. The center-

line of the channel geometry $y = 0$ is a streamline for which $\psi = 0$, $\omega = 0$ and, by symmetry, $v = 0$ and $\partial u / \partial y = 0$.

We choose $P = 0$ at $x = 0$ arbitrarily as a reference pressure value. The fluid temperature at the entrance and the wall (excluding the constriction surface) temperature are maintained at T^*. The constriction surface at $L_1 < x < L_2$ is heated to achieve two limiting thermal conditions, namely constant heat rate $\partial T / \partial y = 0$ and constant surface temperature T at $L_1 < x < L_2$ and $y = b /2$. Constant heat rate problems arise in electric heating, radiant heating, nuclear heating, and in counter-flow heat exchangers when the fluid capacity rates are the same. The constant surface temperature case occurs in evaporators, condensers or any heat exchangers where one fluid has a very much higher heat capacity rate than the other. These two cases cover the usual extremes met in heat exchanger design and are thus of great technical importance.

For a given system of differential equations, many different sets of difference schemes can be formulated. Each set represents a different approximation. The particular choice of difference scheme and the method of its solution as well as the choice of the finite-difference mesh will, in general, determine the consistency, accuracy and convergence of the solution. The practical considerations in making these choices are mostly based on available computer time and storage.

One primary emphasis in this study is on the practical application of numerical methods to the transport problem of separated viscous flow through parallel ducts of complex axial geometries. Proper treatment of the boundary-region flow is essential to the realistic simulation of the separated flow. Of particular importance is the treatment of the flow in the vicinity of the corners Q and R at the two ends of the flow constriction. In response to these considerations, the choice of fine-mesh systems running parallel to the solid walls was made. Considerations of available computational resources led to the choice that the fine grid be restricted to the boundary regions near the two ends only, and that a primary and coarser grid be established in the remaining bulk of the flow region. The network of finite-difference meshes occupying the flow field is shown in Fig. 2. It consists of four grid sizes: $\Delta x_A \times \Delta y_A$, $\Delta x_A \times \Delta y_B$, $\Delta x_B \times \Delta y_A$, and $\Delta x_B \times \Delta y_B$. Accordingly, four difference schemes are formulated for the interior nodes depending upon their location: (i) scheme D for the nodes at $i = k_1$, k_2, ℓ_1 or ℓ_2 and $j = p_1$ or p_2; (ii) scheme C for the nodes at $j = p_1$ and p_2 excluding those corresponding to
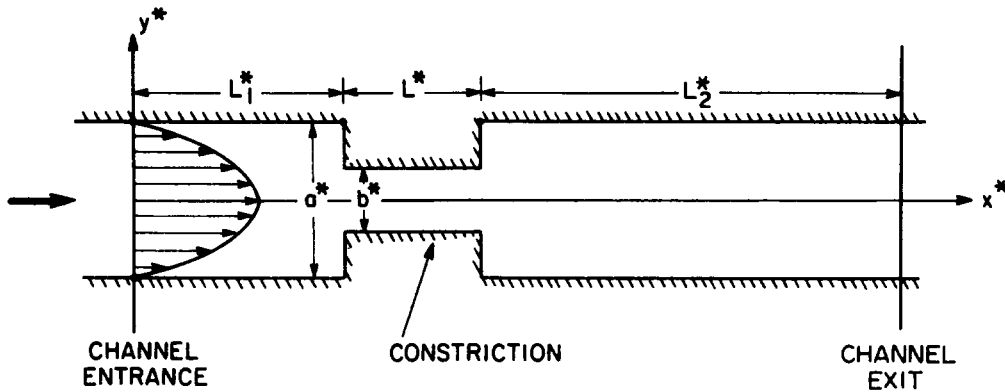
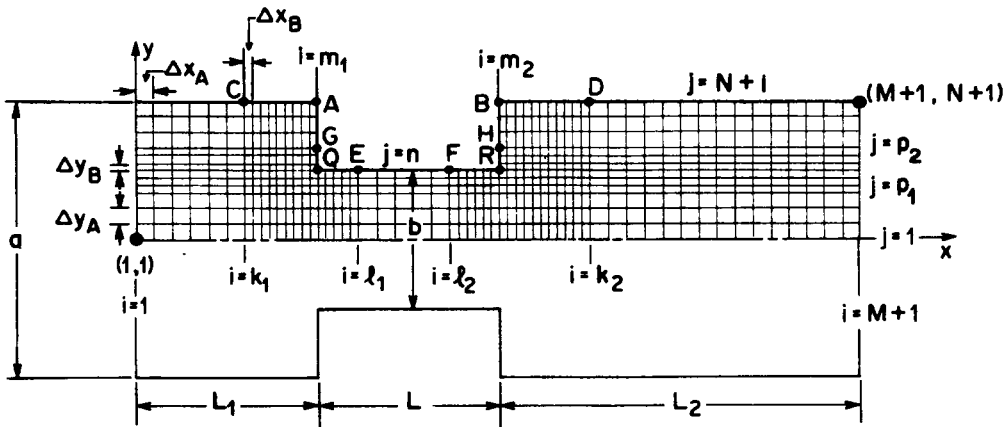Fig. 1. The conduit model configuration and coordinate system.

Fig. 2. Finite-difference meshes

scheme D; (iii) scheme B for the nodes at i = k_1, k_2, ℓ_1 and ℓ_2 excluding those corresponding to scheme D; and (iv) scheme A for all other nodes. In the difference formulation, all variables at the node (i,j) are denoted in the form of $f_{i,j}$. The finite-difference formulas for the derivatives read

(1) scheme A:

$$\frac{\partial f}{\partial x} = \frac{f_{i+1,j} - f_{i,j}}{\Delta x} + O(\Delta x) \qquad \text{(forward)}$$

$$= \frac{f_{i+1,j} - f_{i-1,j}}{\Delta x} + O([\Delta x]^2) \qquad \text{(central)}$$

$$= \frac{f_{i,j} - f_{i-1,j}}{\Delta x} + O([\Delta x]^2) \qquad \text{(backward)}$$

$$\frac{\partial^2 f}{\partial x^2} = \frac{f_{i+1,j} - 2f_{i,j} + f_{i-1,j}}{(\Delta x)^2} + O(\Delta x)^2$$

(ii) scheme B:

$$\frac{\partial f}{\partial x} = \frac{\Delta x_1}{\Delta x_2 \Delta x_{12}} f_{i+1,j} + \frac{\Delta x_2 - \Delta x_1}{\Delta x_1 \Delta x_2} f_{i,j} - \frac{\Delta x_2}{\Delta x_1 \Delta x_{12}} f_{i-1,j} + R'_x$$

$$\frac{\partial^2 f}{\partial x^2} = 2\left(\frac{f_{i+1,j}}{\Delta x_2 \Delta x_{12}} - \frac{f_{i,j}}{\Delta x_1 \Delta x_2} + \frac{f_{i-1,j}}{\Delta x_1 \Delta x_{12}}\right) + R''_x$$

(iii) scheme C:

$$\frac{\partial f}{\partial y} = \frac{\Delta y_1}{\Delta y_2 \Delta y_{12}} f_{i,j+1} + \frac{\Delta y_2 - \Delta y_1}{\Delta y_1 \Delta y_2} f_{i,j} - \frac{\Delta y_2}{\Delta y_1 \Delta y_{12}} f_{i,j-1} + R'_y$$

$$\frac{\partial^2 f}{\partial y^2} = 2\left(\frac{f_{i,j+1}}{\Delta y_2 \Delta y_{12}} - \frac{f_{i,j}}{\Delta y_1 \Delta y_2} + \frac{f_{i,j-1}}{\Delta y_1 \Delta y_{12}}\right) + R''_y$$

Scheme D is the combination of schemes B and C. Here, Δx_{12} and Δy_{12} are defined as $\Delta x_1 + \Delta x_2$ and $\Delta y_1 + \Delta y_2$, respectively. The subscripts 1 and 2 represent the upstream and downstream nodes of (i,j) and thus may correspond to either A and B or B and A, respectively. R' and R'' denote the remainder terms for the first- and second-order derivatives, respectively. The four difference schemes produce four sets of difference equations and boundary conditions covering the entire flow field. Due to space limitation, these finite-difference expressions are not presented here but are available in reference 10.

The following step-by-step iterative procedure is employed for numerical solutions of each interior node, node by node, proceeding downstream from the inlet: at the beginning of the iterative procedure for each interior node; the starting solutions for ω, ψ, u, v, and T must be provided. The use of $f_{i,j} = f_{1,j}$ for generating these starting solutions from those at the channel inlet is found to result in very rapid convergence. The vorticity ω for the new node is determined using the appropriate vorticity equation by the Gauss-Seidel iterative scheme [11], while the stream function ψ of the node is calculated from the appropriate difference formula of Eq. (7) by means of the successive row iteration method [12]. The velocity components u and v at the node are then evaluated from the definition of the stream function, Eq. (6) in difference form. The iteration procedure is terminated when the desired level of convergence in the stream function at each node is attained. After the solutions ω, ψ, u and v for all nodes are calculated, the pressure distribution in the flow field is determined using the momentum equations (4). The difference equation corresponding to (5) is then employed to determine the temperature distributions for both thermal boundary conditions of constant heat rate and constant surface temperature utilizing the Gauss-Seidel iterative scheme. Again, a desired level of convergence is imposed on the temperature solution for the procedure.

Results and Discussion

Computations were carried out using a digital computer for various flow levels in the laminar range up to the transition Reynolds number. For each flow level, the Prandtl number of the fluid was varied to cover gases and common liquids. The ratio of free-flow area to frontal area of the constriction σ was also varied between two limiting values 0 and 1. The channel geometry corresponding to $L = L_1 = L_2/2$ was divided into a grid network of $i = 144$ and $j = 21$ with $\Delta x_A = 3 \frac{1}{3} \Delta x_B$ and $\Delta y_A = 3 \Delta y_B$, in which $L = L^*/L^* = 1.0$, $L_1 = L_1^*/L^*$ and $L_2 = L_2^*/L^*$. The criterion for convergence of ψ and T was set at 0.1 %.

Numerical results were obtained for the loss coefficients K_e and K_c, hydrodynamic and thermal entry lengths, pressure, streamline, velocity and temperature distribution, average Nusselt number Nu and limiting Nusselt number for fully-developed velocity and temperature profiles Nu_∞ for the cases of constant heat rate and constant surface temperature.

Figure 3 illustrates variations of the loss coefficients with the area ratio σ for various Reynolds numbers up to 2000. The results for higher Reynolds numbers obtained through extrapolation are included for completeness.
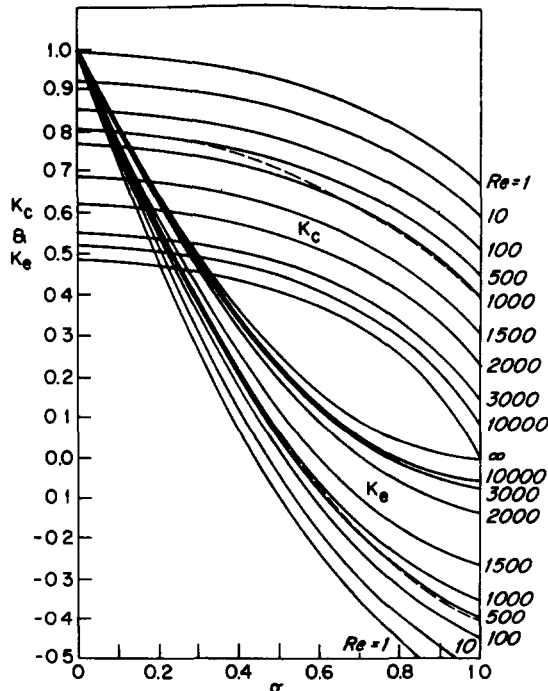

Fig. 3. Loss coefficients K_c and K_e versus area
ratio   (----Kays' semi-empirical result
for laminar flows)

Kays' semi-empirical results for K_c and K_e [2] are shown by a single broken line for the entire laminar regime, Reynolds numbers less than 2000. The inaccuracy of his results is obvious.

Temperature distribution in the flow field at Re = 2000 is shown in Figs. 4 and 5 for constant surface temperature and constant heat rate, respectively. The Prandtl number is varied to determine the effects of thermal diffusivity on thermal stratification in a laminar flow through a heated constriction. All isothermal lines are originated from the inlet of the constriction heated at constant surface temperature, while the constant heat rate case has all isothermal lines originated from the heated constriction surface. For a fluid of low Prandtl number, all isothermal lines in the constriction are short and terminate almost perpendicularly at the channel center line for both thermal boundary conditions. As the Prandtl number increases, these isothermal lines are forced downstream and elongate. At a sufficiently high Prandtl number, high temperature lines terminate at the exit corner of the constriction from which other isothermal lines are originated and extend downstream.

Figure 6 shows the effects of the area ratio σ on thermal-entrance-length Nusselt numbers for the cases of constant heat rate and constant surface temperature at Re = 2000 and Pr = 0.72. It is seen that the combined thermal and hydrodynamic entry length is practically independent of the area ratio and the thermal boundary conditions. The limiting Nusselt number Nu_∞ takes a constant value which is independent of the area ratio: 9.3 and 10.7 for constant surface temperature and constant heat rate, respectively. Both are higher than their counterparts in a long parallel channel flow, 7.54 and 8.235, respectively [1].

The following expressions are derived from the numerical results:

(i) "Critical" constriction length, ℓ_H^*

$$\ell_H^*/D_h^* = 0.065\ Re/\sigma \tag{8}$$

Here, ℓ_H^* is defined as the minimum constriction length beyond which the loss coefficients remain constant and D_h^* is equal to $2b$.

(ii) Combined hydrodynamic and thermal entry length, ℓ_T^*

$$\ell_T^*/D_h^* = C_T Re Pr \tag{9}$$

which is valid for both thermal boundary conditions. The constant C_T has the value of approximately 0.06, which is higher than 0.05 for laminar flow in two parallel planes [1].
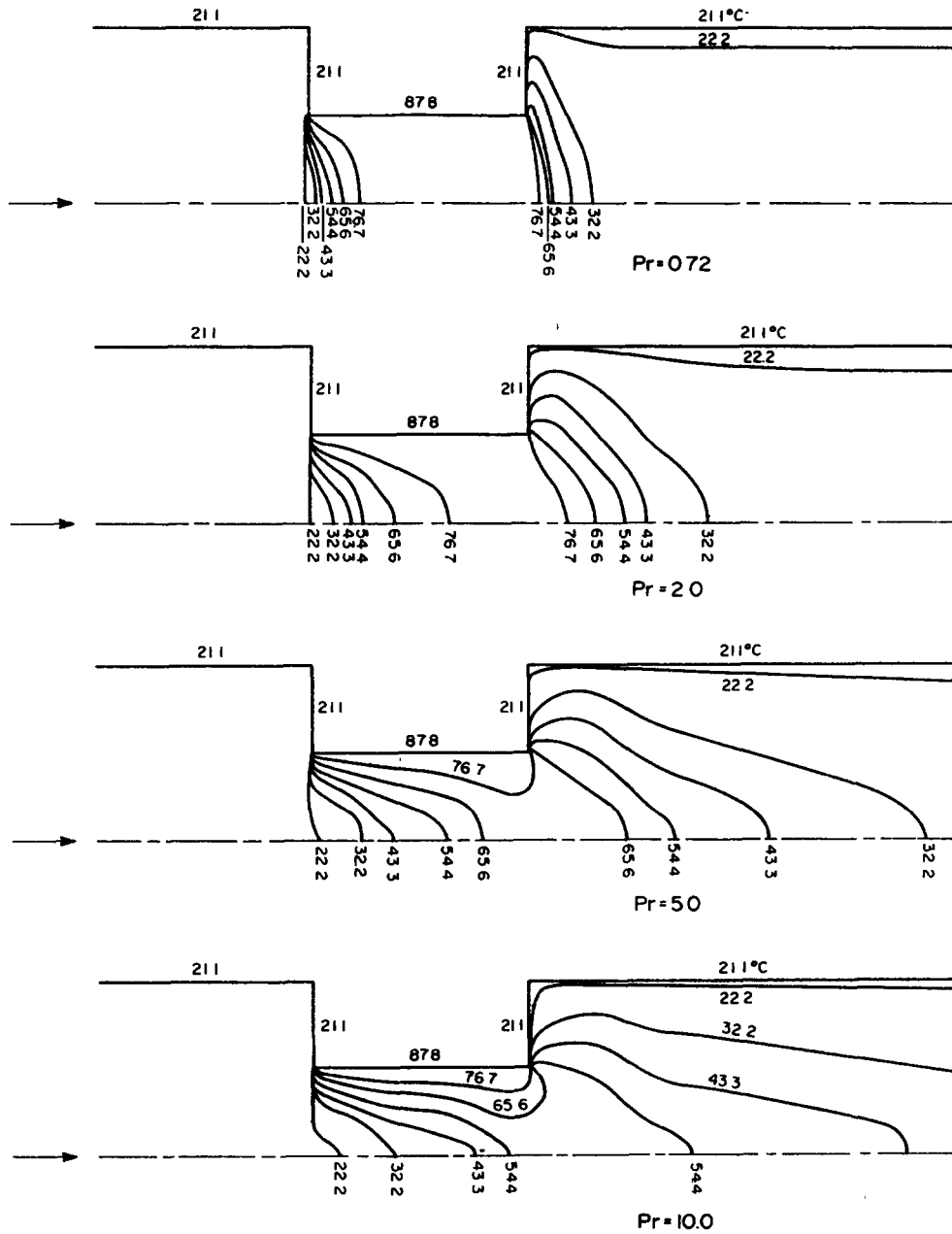
Fig. 4.   Temperature distribution in the constricted parallel channel of
          =0.5 with constant surface temperature, Re=2000 and Pr=0.72,
          2.0, 5.0, 10.

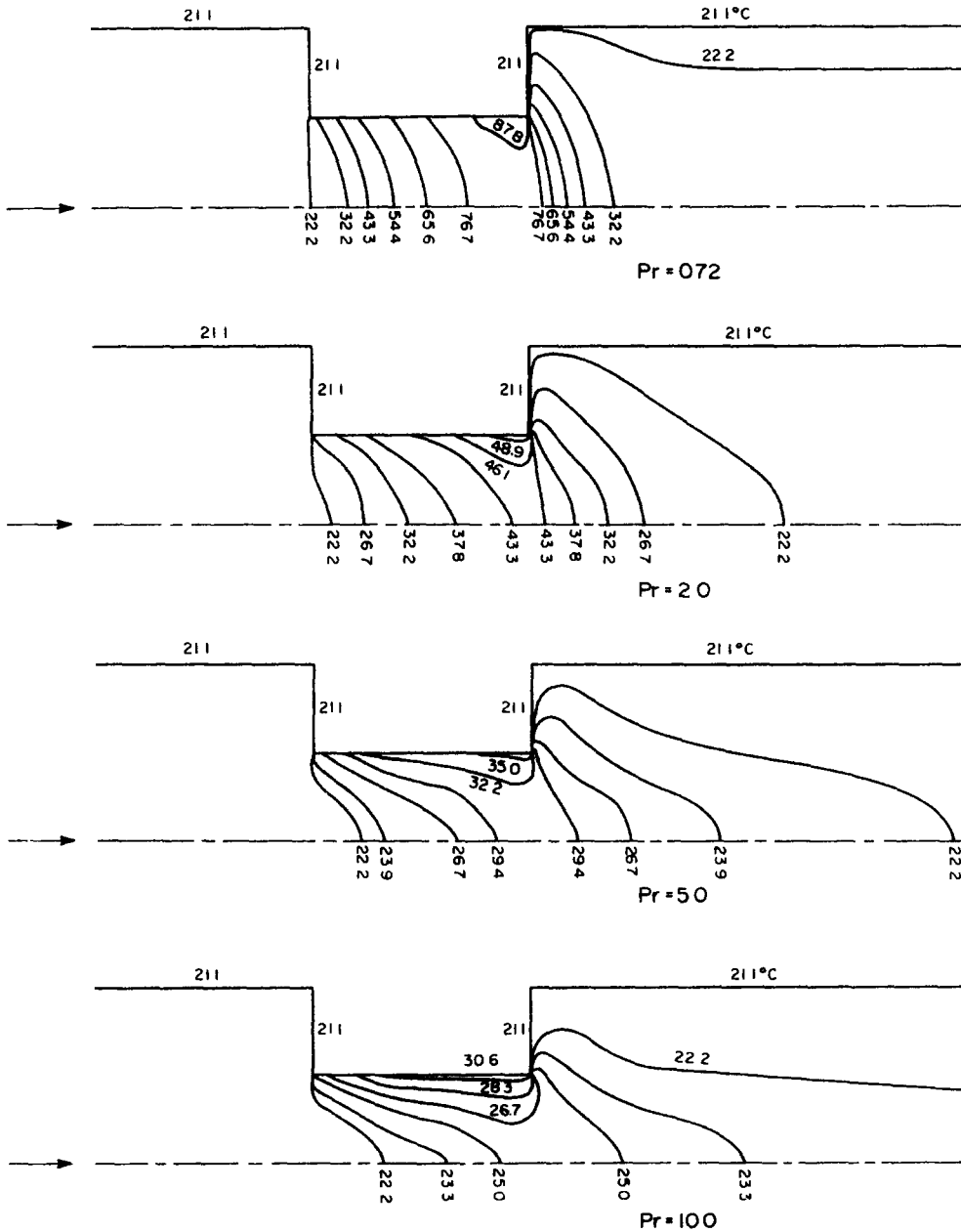Fig. 5.   Temperature distribution in the constricted parallel channel of
          =0.5 with constant heat rate, Re=2000 and Pr=0.72, 2.0, 5.0, 10.0
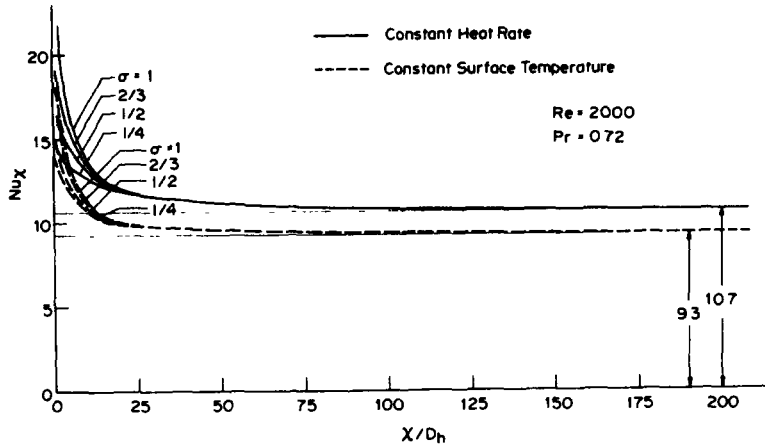
Fig. 6.   Effects of area ratio on thermal-entrance-length
          Nusselt numbers for constant heat rate and constant
          surface temperature cases

(iii)   Average Nusselt number, Nu

$$Nu = 2.26 \, Gz^{1/3} \qquad\qquad Gz > 70 \qquad\qquad (10\text{-}a)$$
$$= 9.3 \qquad\qquad\qquad Gz < 70$$

for constant surface temperature and

$$Nu = 2.60 \, Gz^{1/3} \qquad\qquad Gz > 70 \qquad\qquad (10\text{-}b)$$
$$= 10.7 \qquad\qquad\qquad Gz < 70$$

for constant heat rate, where Gz is the Graetz number defined as $RePrD_h^*/L^*$.
Nu is independent of σ since only sufficiently long constrictions are con-
sidered in the study.   In comparison, laminar flow heat transfer between
parallel planes is theoretically determined as [13]

$$Nu = 1.85 \, Gz^{1/3} \qquad\qquad Gz > 71.4$$
$$= 7.6 \qquad\qquad\qquad Gz < 71.4$$

and

$$Nu = 1.99 \, Gz^{1/3} \qquad\qquad Gz > 71.4$$
$$= 8.24 \qquad\qquad\qquad Gz < 71.4$$

for constant surface temperature and constant heat rate, respectively.   A
variation in flow cross-sectional area in parallel ducts causes an enhance-
ment in laminar-flow heat transfer, as expected.

Conclusions

Numerical analysis has been performed on laminar transport phenomena in parallel ducts with a long constriction. The numerical scheme is distinguished in two respects: (i) capable of treating high velocity flows up to the transition Reynolds number and (ii) no restriction imposed on the velocity profile at the channel exit. Figure 3 determines the loss coefficients due to abrupt contraction and enlargement. It is concluded that (i) The "critical" constriction length, combined hydrodynamic and thermal entry length and average Nusselt numbers in the constriction can be predicted by Eqs. (8), (9) and (10), respectively; (ii) The area ratio affects the hydrodynamic entrance length and the local Nusselt number near the constriction inlet but not the thermal entry length and the average Nusselt number, and (iii) The flow constrictions cause a substantial augmentation in heat transfer performance.

References

1.   W.M. Kays, Convective Heat and Mass Transfer, McGraw-Hill Book Co., New York (1966).

2.   W.M. Kays, Trans. ASME 72, 1067 (1950).

3.   R.P. Benedict, N.A. Carlucci, and S.D. Swetz, J. of Engineering for Power, Trans. ASME, 88A, 73 (1966).

4.   R.P. Benedict, ibid., 67 (1966).

5.   D. Greenspan, Int. J. for Numerical Methods in Engineering 6, 489 (1973).

6.   M.D. Olson, in R.H. Gallagher, J.T. Oden, C. Taylor, and O.C. Zienkiewicz (eds.), Finite Elements in Fluids, 1, Viscous Flow and Hydrodynamics, John Wiley, p. 69 (1975).

7.   D.F. Young, J. of Engineering for Industry, Trans. ASME 90B, 248 (1968).

8.   B.D. Seeley, M.S. Thesis in Biomedical Engineering, Iowa State University, Ames, Iowa (1975).

9.   N.V. Gillani and W.M. Swanson, J. of Fluid Mechanics 78, pt. 1, 99 (1976).

10. S. Bunditkul, Ph.D. Thesis in Mechanical Engineering, University of Michigan, Ann Arbor, Michigan (1977).

11. J. Fromm, A Method for Computing Nonsteady, Incompressible, Viscous Fluid Flows, Los Alamos Scientific Laboratory, Los Alamos, New Mexico (Sept. 1963).

12. G.H. Brace, D.W. Peaceman, H.H. Rachford, Jr., and J.D. Rice, Petroleum Transactions, Amer. Inst. of Mining & Metallurgical Engrs. 198, 79 (1953).

13. J.G. Knudsen and D.L. Katz, Fluid Dynamics and Heat Transfer, McGraw-Hill, New York, chaps. 9 and 13 (1958).